TOPOMAPPING OF MARS WITH HRSC IMAGES, ISIS, AND A COMMERCIAL STEREO WORKSTATION

R. L. Kirk, E. Howington-Kraus, D. Galuszka, B. Redding, T.M. Hare

U.S. Geological Survey, Flagstaff, AZ 86001, USA - rkirk@usgs.gov

Commission 1V, WG IV/7

KEY WORDS: HRSC, Mars, DTM, photogrammetry, photoclinometry, shape-from-shading, extraterrestrial mapping

ABSTRACT:

We demonstrate that the freely available USGS planetary cartography software package ISIS and the commercial photogrammetric software SOCET SET jointly provide a complete environment for the processing of Mars Express High Resolution Stereo Camera (HRSC) images. Capabilities include bundle adjustment, automated production and interactive editing of stereo digital terrain models (DTMs), orthomosaic production, photometric modeling and normalization, and DTM refinement by photoclinometry/shape-from-shading. The generation of DTMs and other products for two test areas on Mars is described; a companion paper by Heipke et al. (2006) compares DTMs produced from these test datasets by multiple investigators using alternate approaches. SOCET SET capabilities relevant to multi-line scanners (including HRSC) are evolving, and improved performance in several areas can be expected in the near future. ISIS by itself provides useful capabilities for orthomosaic production with pre-existing DTMs, photometry, and photoclinometry, and the value of these free tools will be increased once an HRSC bundle-adjustment capability is implemented.

1. INTRODUCTION

HRSC on Mars Express (Neukum et al., 2004) is the first camera designed specifically for stereo imaging to be used in mapping a planet other than the Earth. Nine detectors view the planet through a single lens to obtain four-band color coverage and stereo images at 3 to 5 distinct angles in a single pass over the target. The short interval (tens of seconds) between acquisition of the successive images ensures that the surface, atmosphere, and lighting conditions will be unchanged, minimizing problems in comparing the stereo images. The resolution of the nadir channel is 12.5 m at periapsis, poorer at higher points in the elliptical orbit. The stereo channels are typically operated at 2x coarser resolution and the color channels at 4x or 8x. Since the commencement of operations in January 2004, approximately 58% of Mars has been imaged at nadir resolutions better than 50 m/pixel. This coverage is expected to increase significantly during the recently approved extended mission of Mars Express, giving the HRSC dataset enormous potential for regional and even global mapping.

Systematic processing of the HRSC images is carried out at the German Aerospace Center (DLR) in Berlin, by using the VICAR software system (Scholten et al., 2005). This processing includes decompression of the images, radiometric calibration, orthorectification (i.e., projection into map coordinates allowing for topographic parallax) based on elevations from MOLA altimetry (Smith et al., 2001), and production of preliminary stereo DTMs at 200 m/post plus images orthorectified with these DTMs. The resulting standard products are referred to as Levels 1, 2, 3, and 4 respectively (note that these correspond to Levels 0, 1, 2, and 2 as generally referred to in ISIS processing (Batson, 1995); ISIS refers to map-projected products as Level 2 regardless of the DTM data used for rectification). These products are generated systematically, in near-real time for all orbits, though only the HRSC Level 2 and (more recently) Level 3 products are being archived. The trade-off of universal coverage but limited DTM resolution makes these products optimal for many but not all research studies. Experiments on adaptive processing with the same software (Gwinner et al., 2005; 2006) have shown that DTMs of higher resolution (down

to 50 m/post) can be produced. Systematic production of DTMs by this approach, followed by archival of the resulting, definitive Level 4 products, is now envisioned. In addition, numerous Co-Investigators on the HRSC team (including ourselves) are actively researching techniques to improve on the standard products, by such methods as bundle adjustment, alternate approaches to stereo DTM generation, and refinement of DTMs by photoclinometry (shape-from-shading) (Albertz et al., 2005). The HRSC team is conducting a systematic comparison of these alternative processing approaches by arranging for team members to produce DTMs in a consistent coordinate system from a carefully chosen suite of test images (Heipke et al., 2006). Here we describe our own approach to HRSC processing and the results we obtained with the test images.

2. PROCESSING APPROACH

We have developed an independent capability for processing of HRSC images at the USGS, based on the approach previously taken with Mars Global Surveyor Mars Orbiter Camera (MGS MOC) images (Kirk et al., 2003b). The chosen approach uses both the USGS digital cartographic system ISIS and the commercial photogrammetric software SOCET SET (® BAE Systems) and exploits the strengths of each. This capability is almost entirely independent of the other approaches being compared by Heipke et al. (2006), several of which make use of the mission-supplied bundle-adjustment results and the VICAR stereo matching software. It thus provides an interesting point of comparison for the test. More importantly, it prepares us for systematic mapping with HRSC data, and makes some useful processing tools (including relatively powerful photometric normalization and photoclinometry software) available to a wide community of ISIS users.

ISIS (Eliason, 1997; Gaddis et al., 1997; Torson and Becker, 1997) provides an end-to-end system for the analysis of digital images and production of maps from them that is readily extended to new missions. Its stereo capabilities are, however, limited. SOCET SET (Miller and Walker, 1993; 1995) is tailored to aerial and Earth-orbital imagery but provides a

complete workflow with modules for bundle adjustment (MST), automatic stereomatching (ATE), and interactive quality control/editing of DTMs with stereo viewing (ITE). Our processing approach for MOC and other stereo datasets has been to use ISIS to ingest images in an archival format, decompress them as necessary, and perform instrument-specific radiometric calibration. Software written in ISIS is used to translate the image and, more importantly, orientation parameters and other metadata, to the formats understood by SOCET SET. The commercial system is then used for "three-dimensional" processing: bundle-adjustment (including measurement of needed control points), DTM generation, and DTM editing. Final steps such as orthrectification and mosaicking of images can be performed either in SOCET SET or in ISIS after exporting the DTM data back to it. This workflow was modified slightly for HRSC to take advantage of the DLR processing pipeline. As the first step in DTM production, we use the ISIS program *mex2isis* to import VICAR Level 2 files into ISIS where they can immediately be used (e.g., orthorectified based on MOLA or other pre-existing DTM data by using the program *lev1tolev2*) or exported to SOCET SET. HRSC Level 3 and 4 products can also be imported with *mex2isis* and used as map-projected data (e.g., Level 4 DTMs from DLR can be compared with those made in SOCET SET).

The importation of Level 2 images includes reformatting needed to accommodate limitations common to the sensor models (software that calculates the transformation between image coordinates and world coordinates) used in ISIS and SOCET SET. SOCET SET includes "generic" sensor models for both pushbroom scanners and framing cameras. The HRSC scanner and Super-Resolution Channel (SRC) images can be used with these models, respectively, once the interior orientation parameters are made available in the appropriate format, and a significant advantage of the system is that scanner and frame images can be freely mixed in the bundle-adjustment and DTM generation steps. For example, it is possible to produce DTMs from SRC data in combination with MOC narrow-angle scanner images, which have comparable resolution (Albertz et al., 2005). ISIS sensor models for HRSC and SRC were developed by adapting existing code for cameras with similar properties. Both of the scanner models we use make the simplifying assumption that the integration time is the same for every line of an image, but HRSC scanner images can have different exposure times for different lines, as recorded in VICAR line prefixes. Blocks of consecutive lines with constant exposure time are therefore identified and formatted as separate ISIS images. One line of overlap is provided between successive blocks so that they can be tied together during bundle adjustment. If necessary, the blocks are split into files small enough to be compatible with operating systems using 32-bit addressing. SRC images, which are provided in various cropped formats, are padded out to a fixed size corresponding to the full detector array.

3. DATASETS FOR DTM COMPARISON

The comparison process, which is described in more detail by Heipke et al. (2006), consists of test images, specifications for products to be generated by test participants, and procedures for evaluation of the products. Two datasets have been chosen as the basis for the initial comparisons reported here; other areas may be mapped in the future. These are a single image set from orbit h1235 and a block of three adjacent images from h0894, h0905, h0927. The area of interest in h1235 covers western Candor Chasma (-8° to -4°N, ~282° to 284°E) at a nadir resolution of 27 m/pixel and includes the spectrally distinctive Ceti Mensa. This region contains steep slopes on the walls

bounding the chasma, as well as expanses of plateau with very little image texture. The second dataset covers heavily cratered terrain including the system of sinuous channels known as Nanedi Valles (test area 2.5° to 7.5°N, 310° to 314°E) at 12 to 15 m/pixel. In addition to being scientifically interesting, this area provides a test of capabilities for producing seamless DTMs from blocks of images by bundle adjustment. The camera was operated somewhat differently during the collection of the two test datasets, with significant consequences for our processing efforts. In orbit h1235 a relatively short line integration time was used, resulting in oversampling of the images along track by a factor of roughly two. For example, the nadir image has a ~27 m square pixel footprint but ~11 m along-track spacing within the test area. The integration time was held constant over a substantial arc of the orbit, permitting us to map the entire test area with a single image file for each channel. Data acquisition over the second test area was much more representative of typical HRSC operations: the line integration time was chosen to yield a pixel spacing close to the pixel footprint dimensions. Because of the eccentricity of the Mars Express orbit, the line time was adjusted frequently to maintain the consistency between the pixel scale and along-track spacing. As a result, we were forced to break the data for each channel into an average of 8 constant-line-time files over the latitude range of the test area. This multiplicity of files significantly impacted both bundle adjustment and DTM collection.

Output products for the comparison have been produced in IAU/IAG 2000 coordinates (Seidelmann et al., 2002) with planetocentric latitude and east longitude. For simplicity, elevations are referred to a sphere of radius 3396.0 km rather than to an equipotential system. DTM products are produced in sinusoidal projection with specified center longitude for each test area, but each test participant is free to choose an appropriate grid spacing.

4. RESULTS

4.1 Bundle Adjustment

Additional limitations arise because the capability of SOCET SET to deal with multiline stereo scanners such as HRSC is evolving rapidly. A major strength of this type of camera is that the orientations of the different image channels are not independent, but are rigidly related to one another and follow the common trajectory of the spacecraft. Introduction of the appropriate constraints between the orientation histories of the channels into the bundle adjustment will increase the robustness of the result and decrease the amount of ground control needed by eliminating the physically impossible relative motions of the channels. Unfortunately, the version of SOCET SET (5.2) used for the work reported here does not allow for the introduction of such constraints, although the capability existed in earlier versions and has since been reintroduced in SOCET SET 5.3. We therefore adjusted the position and pointing histories of each image channel independently. The adjustment included positional biases and linear drifts (i.e., velocity biases) with respect to the nominal spacecraft trajectory in the in-track, cross-track, and radial directions, and fixed biases only to the three orientation angles.

Point Type	Number	Horizontal (m)	Vertical (m)
		Weights	
XYZ Control	7	50–75	20–50
Z Control	17	10000	10–40
Tie	7	10000	10000
		RMS Residuals	
All	31	185.02	14.60

Table 1. Candor Chasma h1235 control points and ground residuals.

Table 1 summarizes the control point data collected for orbit h1235 in the Candor test area. The points were measured on all seven simultaneously adjusted channels (nadir, two stereo, and four color). Placement of the manually selected control points was found to be critical; matching MOLA to the images to constrain horizontal coordinates is easiest at slope breaks such as the canyon edges, but vertical constraints are best obtained in areas of low slope. As a result, it is preferable to choose separate points for horizontal or XYZ and for purely vertical control. It is also useful to import the MOLA ground tracks into SOCET SET in order to be sure of picking control points on or near altimetry profiles rather than in gaps where the MOLA DTM has been filled by interpolation. The tightest vertical weighting corresponds to the absolute vertical accuracy of MOLA (Smith et al., 2001); points farther from MOLA tracks were weighted more loosely. The horizontal weighting was chosen to approximate the HRSC pixel scale (Table 2). The RMS vertical residuals are consistent with the weighting but the horizontal residuals are higher, probably as a consequence of the 463 m/post MOLA grid spacing.

Image	Sample Spacing (m)	Line Spacing (m)	Samp RMS (pixels)	Line RMS (pixels)	Total RMS (Pixels)
S1	50.0	25.8	0.692	0.541	0.878
IR	202.9	101.3	0.420	0.373	0.561
GR	214.5	93.0	0.548	0.393	0.675
ND	27.3	11.3	0.550	0.274	0.615
BL	222.4	88.4	1.165	0.725	1.372
RE	244.3	161.4	0.598	0.286	0.663
S2	62.8	18.9	0.450	0.447	0.634

Table 2. Candor h1235 bundle adjustment residuals in image space. Pixel spacings are calculated at 5.44°S, 76.25°E, within the test area.

Table 2 shows the image-space residuals for each channel, as well as two measures of image resolution. The sample spacing is set by the instantaneous field of view, whereas the line spacing is determined by the integration time and spacecraft velocity. Subpixel RMS residuals were obtained for all channels except the blue, which has by far the poorest signal to noise ratio and is strongly affected by compression artifacts. Table 3 lists the position, velocity, and angular biases obtained in the adjustment, along with the weights assigned. These were based on the a priori accuracy of the orientation data (Albertz et al., 2005), except that we inadvertently used 0.25° in place of the correct value of 0.025°. The extreme values are roughly 3 times the corresponding weights, but there is very little consistency between the adjustments for different channels. This is likely the result of the strong correlations between position and pointing corrections for a single, independently adjusted channel, along with our overly loose weighting of the angles. Enforcement of consistent adjustment for all channels would greatly reduce this correlation and would result in more physically meaningful results.

Because of the large number of constant-line-time segments for each image in the Nanedi test area, we adjusted only the nadir and stereo channels. Images from orbit h0927 could not be adjusted successfully; stereopairs of the adjusted segments displayed large and spatially varying amounts of y-parallax. This orbit was therefore omitted from bundle adjustment and subsequent processing. The reason for this behavior is not understood but may be related to the larger roll angle for this

orbit, 5° as compared to ~1° for the others. Our approach of dividing the HRSC images into segments of course requires that the segments be adjusted consistently, in order to obtain physically meaningful results and seamless DTMs. We attempted to do this by making use of an older version of SOCET SET (4.4) in which constrained bundle adjustment was (nominally) possible. We first attempted to constrain all image channels to adjust together, but extremely large RMS residuals (~10 pixels) and y-parallaxes resulted. We therefore attempted constraining the segments of each channel to adjust consistently with one another, but removed the constraints between channels. This resulted in convergence of the adjustment to a solution with low residuals, negligible y-parallax, and consistency between the various stereopairs of image segments and MOLA, at least to first order. The results of DTM collection, described below, make it clear that the adjustments were not truly consistent between image segments as desired, and imply that the SOCET SET 4.4 version of constrained adjustment does not function correctly. Because of the problems with the Nanedi bundle adjustment, we omit the detailed statistical results. Constrained adjustment has been reintroduced in the latest version (5.3) but we have yet to test whether correctly constrained solutions for HRSC can be obtained. An alternative approach to obtaining consistent adjustment of the image segments would be to place tie points (weighted heavily in image space, very loosely in ground space) in the one line of overlap between each pair of successive segments.

4.2 DTM Collection

The SOCET SET stereomatching module, ATE, uses a multi-pass, multi-resolution strategy based on image correlation and outputs elevations at DTM grid points or TIN points (Zhang and Miller, 1997). Intermediate results that would be of interest for the HRSC DTM comparison, such as matched image coordinates or ungridded ground point coordinates, are not accessible. ATE includes a capability for multi-way image matching, which is implemented by performing all possible pairwise comparisons between the images at a given horizontal location, and choosing the result with the highest correlation coefficient. Unfortunately, a bug in recent versions of SOCET SET causes on-the-fly epipolar rectification, which is needed for multi-way matching, to fail for scanner images. The bug will be corrected in a future release of SOCET SET, making multi-way matching possible. This is expected to improve the robustness of DTM generation and reduce the need for interactive editing.

As a workaround, we pre-rectified each pair of images (nadir-stereo1, nadir-stereo2, and stereo1-stereo2) and collected a separate DTM from each pair. We collected DTMs at 75 m/post in the interior of Candor Chasma and 300 m on the walls and surrounding plateau, and merged the results from both spacings and all 3 image combinations at 75 m/post. The latter spacing, approximately 3 times the nadir pixel scale, was chosen as a practical lower limit on DTM resolution for area based matching (3 pixels is the smallest possible odd-dimensioned matching patch). The larger spacing results in

	IT position bias (m)	CT position bias (m)	Rad position bias (m)	IT velocity bias (m/s)	CT velocity bias (m/s)	Rad velocity bias (m/s)	Omega bias (°)	Phi bias (°)	Kappa bias (°)
Weight	1000	1000	1000	1	1	1	0.250	0.250	0.250
S1	-1418.7	-1429.7	-66.8	-0.15	-0.19	0.13	0.143	0.527	0.544
IR	189.5	-1021.5	363.2	0.10	-0.16	0.02	0.138	0.676	0.435
GR	-819.1	-875.0	198.7	-0.03	-0.05	0.02	0.170	0.571	0.049
ND	-1565.3	-2422.2	453.9	-0.02	0.06	0.13	0.304	0.510	-0.046
BL	687.4	-661.8	107.5	-0.07	0.78	0.44	0.129	0.696	-0.167
RE	1212.1	-338.5	-176.0	0.53	0.44	0.54	0.034	0.745	-0.441
S2	-537.2	-1982.7	784.0	-1.26	0.26	-0.09	0.126	0.590	-0.556

Table 3. Solved parameters of the Candor h1235 bundle adjustment. IT, CT, Rad indicate in-track, cross-track, and radial coordinates; omega, phi, and kappa are rotations around the in-track, cross-track, and radial axes respectively.
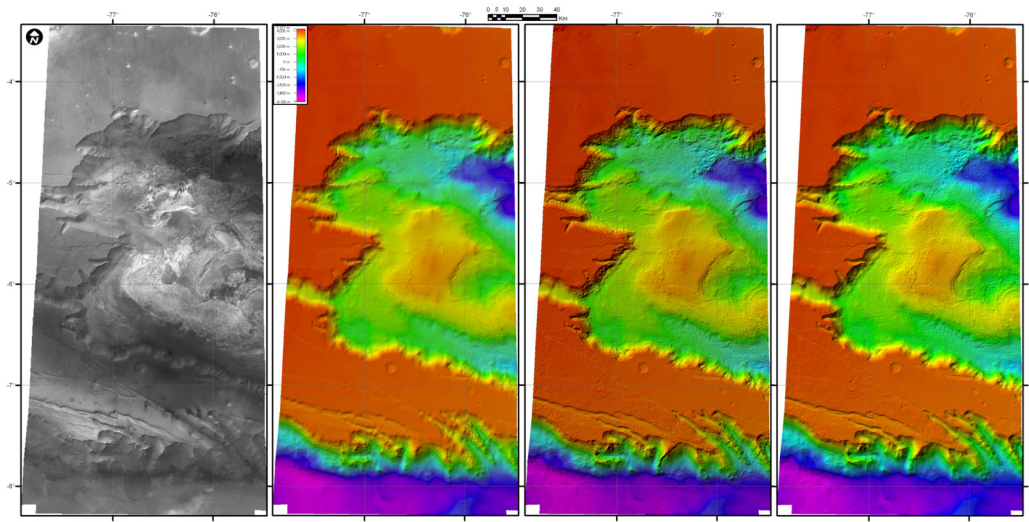
Figure 1. Color-coded shaded relief maps of the Candor Chasma test area (orbit h1235). From left to right, orthorectified HRSC nadir image, MOLA global DTM data, USGS HRSC stereo DTM, and USGS HRSC DTM refined by photoclinometry/shape-from-shading.

decreased matching artifacts in steep and bland areas. A small amount of interactive editing was performed to remove areas of obvious matcher errors from the individual DTMs before they were merged. In most cases, this resulted in the combined DTM being based on the other, more successful matching results. Parts of the plateau around Candor Chasma, which has very little image texture, could not be matched successfully and were filled with MOLA data. The effort required to generate the Candor DTM included 6.2 hours of computer time on a 1.5 GHz Sun Blade 1500 workstation for matching and 56 hours of interactive work for preparing the images and setting up and merging the multiple DTMs. The resulting DTM is shown in Figure 1. As would be expected, the 75 m/post stereo DTM appears sharper than either MOLA at 463 m/post or the preliminary HRSC DTM at 200 m/post (Figure 2). The added detail is subjectively well correlated with the image but is not crisp at the single-post scale. This must in part be a result of the poorer resolution of the stereo channels compared to the nadir. The RMS amplitude of the local variations in the DTM, in an area of the canyon interior where the images show a relatively smooth surface, is approximately 17 m. If these variations can be taken as an indication of the local vertical precision of matching, then a RMS matching precision of 0.185 pixel has been achieved. The absolute errors are affected by the results of the bundle adjustment and other systematic effects, and are, of course, considerably larger. Heipke et al. (2006) have compared the stereo DTM with collocated MOLA measurements (individual points rather than gridded data) and report a mean difference of 48.5 m and standard deviation of 120 m along a pair of MOLA profiles. This comparison includes points on the steep canyon walls, where the MOLA-HRSC differences are greatest and most sensitive to resolution effects and horizontal misalignment as well as matching errors.

relief with corresponding illumination, computed from MOLA DTM (resampled from 463 m/post), DLR preliminary HRSC DTM (resampled from 200 m/post) and USGS HRSC DTM (75 m/post).

For Nanedi Valles, which lacks the extremely steep or flat areas encountered in Candor, DTMs were collected over the full study area at both 75 and 300 m/post, although the higher resolution of these images would support a grid spacing on the order of 50 m. DTMs obtained from the various segments of a given pair of HRSC channels were first merged, and then the DTMs for the various channel pairs and grid spacings were edited and merged as for Candor Chasma. The effort required to make the Nanedi DTM was 11.5 hours of computer time for matching and 53 hours of interactive work. The results (Figure 3) clearly indicate the failure of the bundle adjustment to achieve consistency between the successive segments of each image channel; the composite DTM shows discontinuities between

Figure 2. Comparison of DTM details for 22.5x18.75-km subareas on the rim of Candor Chasma (top) and on the interior deposit Ceti Mensa (bottom). From left to right in each row, HRSC nadir image and shaded
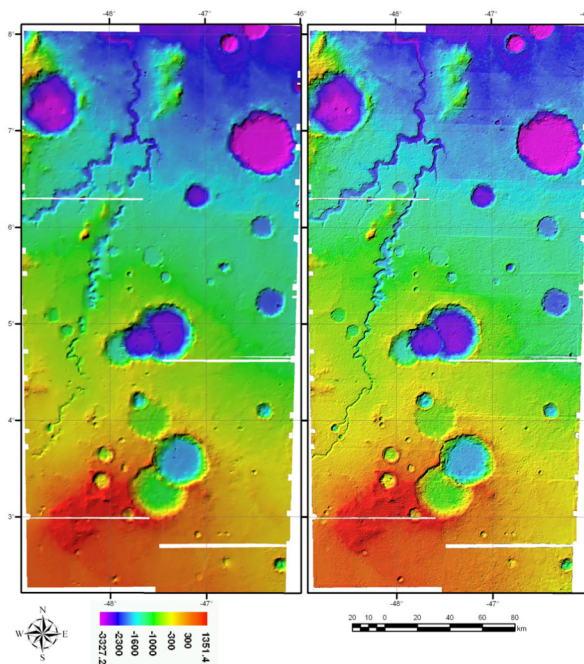
Figure 3. Color-coded shaded relief maps of the Nanedi Valles test area (orbits h0894, h0905 only) from MOLA (left) and USGS HRSC DTM (right). Improved detail of HRSC DTM is evident even at this scale, particularly within the channel system. Discontinuities (mainly running east-west) result from inconsistent bundle adjustment of the constant-
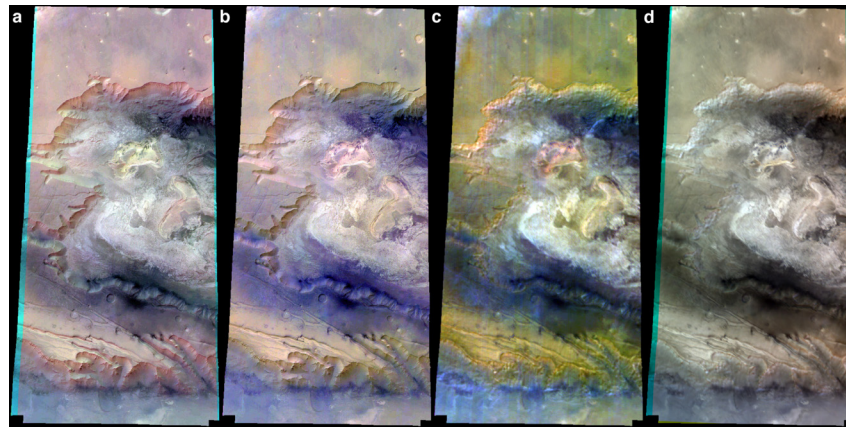
Figure 4. Examples of ISIS cartographic and photometric processing of Candor h1235 images orthorectified with stereo DTM. (a) RGB composite of infrared, red, and green channels, pan-sharpened with nadir. (b) Equivalent pan-sharpened composite of red, green, and blue channels. (c) Color-albedo map of red, green, and blue channel data with atmospheric haze subtracted, topographic shading (based on DTM) divided out, and local shading errors suppressed by lowpass filtering. (d) Equivalent RGB composite of albedo maps from the stereo1, nadir, and stereo2 panchromatic channels, showing phase-angle dependent differences in scattering as color differences.

line-time segments of the images. Gaps occur where edge effects prevented stereo matching around the perimeter of each segment pair and fill data were unavailable from other image combinations.

the areas collected from different pairs of image segments, as well as long-wavelength tilts relative to MOLA within each such area. Gaps in the composite DTM result because of edge effects in the matching algorithm: each segment DTM contains unusable points around its margin, and in the merged dataset these areas may or may not be filled with data from other combinations of image segments. On a more positive note, the higher image quality and less extreme terrain in this area result in better success of the automatic matching process, and the mismatches between DTM data from the adjacent orbits are less severe than those between orbit segments, suggesting that mapping of blocks of orbits will proceed smoothly once the problems with the bundle adjustment step are resolved.

4.3 ISIS Cartographic Processing

With the DTM and orthorectified images translated back into ISIS format, a variety of useful additional processing steps could be demonstrated, such as generation of pan-sharpened false and true color images, color-albedo maps, and band-ratio images with correction for surface and atmospheric photometric effects (Figure 4). The albedo maps were produced by subtracting a constant contribution of atmospheric haze from each image and dividing by a synthetic image generated by relief shading of the DTM based on a realistic (non-Lambertian and phase-dependent) photometric function (Kirk et al., 2003a). The haze values were estimated by the intercept of a linear regression between image and synthetic image over a region of canyon wall, chosen to have minimum albedo variations and maximum topographic shading. The photometrically corrected image contains artifacts caused by the errors and limited resolution of the DTM as well as actual albedo variations. It was therefore lowpass filtered to isolate the albedo variations over lengthscales greater than about 2 km. Similar processing of the nadir and stereo panchromatic images, which have phase angles ranging from 17° to 48°, reveals a surprising diversity of surface photometric behavior (Figure 4c). Maps of phase dependence of scattering will not only be useful for empirical classification of surface units and quantitative modeling of microtexture and other photometric parameters, they are also likely to be essential for the rigorous comparison of the color images, which span a comparable range of phase angles.

Finally, by dividing the nadir image by the smoothed albedo map, we obtained an image in which all but the most localized albedo variations had been removed. The albedo-corrected

image was then analyzed by two-dimensional photoclinometry (Kirk, 1987) to generate a DTM that contains real geomorphic detail at the limit of image resolution (Figure 5) while retaining consistency with the stereo and MOLA data over longer distances (Fig. 1). Without the albedo correction based on the stereo DTM such a result would be unachievable because of the extremely strong albedo contrasts in the test area. Because photoclinometry serves merely as a form of "smart interpolation" to fill in local details in the stereo DTM, the complications that can arise in the general case (Kirk et al., 2003a) do not occur, and this processing can be carried out unsupervised.
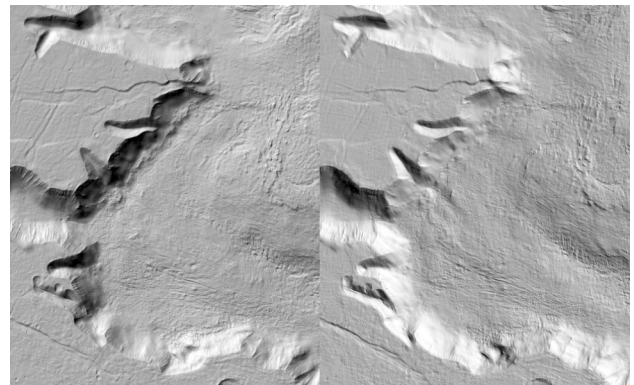
Figure 5. Shaded relief of 73x90-km subarea of photoclinometry-enhanced Candor DTM. Left: with illumination matching HRSC image. Right: illuminated from upper right, 90° different sun azimuth.

4.4 Future Work

In the near future, we will test the reinstated capability for constrained bundle adjustment in SOCET SET 5.3 on both the Candor image set (constraining channels only) and that for Nanedi (constraining first segments of channels, then all segments of all channels). If successful, constrained adjustment should be stable with fewer measured points, thus reducing the effort needed to control the images, and will also yield more physically meaningful adjusted orientation values. Processing of orbits with frequent changes of line integration time (i.e., the majority of HRSC data) should then yield DTMs without the discontinuities caused by the inconsistent adjustment reported here. The effort needed to collect and merge a large number of small DTM sections will still be substantial, however, and loss of data around the edges of each stereopair may still lead to gaps in the merged DTM. We therefore plan to modify both the ISIS and HRSC sensor models to accommodate images in which the integration time changes; an agreement previously

negotiated between the USGS and BAE Systems permits us to modify the sensor code for our use (and that of other planetary researchers) with Mars data, and gives BAE the option of distributing the modified code in the future. The VICAR to ISIS and ISIS to SOCET translation steps will be correspondingly modified to propagate the needed integration time information. When the bug that prevents on-the-fly rectification of scanner images is fixed in a future release of SOCET SET, we will re-collect the Candor and Nanedi DTMs in order to test the capability for multi-image matching. This capability will certainly reduce the time required to set up and merge multiple DTMs. It is to be hoped that multi-way matching will also be less susceptible to blunders than pairwise matching, reducing the need for interactive editing of the resulting DTM.

5. CONCLUSIONS

We have demonstrated that ISIS and the commercial stereo-analysis package SOCET SET together enable a complete workflow for producing stereo DTMs, orthoimages, and derived products from HRSC images of Mars. This combination of software includes capabilities such as multi-sensor bundle adjustment and matching, interactive quality control and DTM editing, and two-dimensional photoclinometry/shape-from-shading that may be absent or less well developed in some other HRSC processing environments. Several bugs and limitations were identified with recent versions of SOCET SET that temporarily restrict its ability to take full advantage of the multi-line design of HRSC, but these problems are being corrected. We therefore expect that it will be possible in the near future to obtain results superior to those reported here with significantly reduced effort. This opens the way for the USGS and other users with the resources to obtain the commercial software to begin systematic regional or even global topomapping of Mars with HRSC data, should such mapping be desired in support of future research and mission operations. Users who cannot afford a commercial stereo system also stand to benefit. We conclude by noting that orthorectification of the images, photometric normalization and modeling, and photoclinometry are all performed with the free software system ISIS. Although SOCET SET was used for bundle adjustment in this study, the USGS is currently developing its own bundle adjustment software for HRSC and other line scanners, which, when available, will make it possible for ISIS users to control HRSC images to MOLA and therefore to perform many of the processing and analysis steps described here by using MOLA topographic data.

6. REFERENCES

Albertz, J., Attwenger, M., Barrett, J. M., Casley, S., Dorninger, P., Dorrer, E., Ebner, H., Gehrke, S., Giese, B., Gwinner, K., Heipke, C., Howington-Kraus, E., Kirk, R. L., Lehmann, H., Mayer, H., Muller, J.-P., Oberst, J., Ostrovskiy, A., Renter, J., Reznik, S., Schmidt, R., Scholten, F., Spiegel, M., Stilla, U., Wählisch, M., Neukum, G., and HRSC Team, 2005. HRSC on Mars Express—Photogrammetric and cartographic research. *Photogrammetric Engineering & Remote Sensing*, 71(10), pp. 1153–1166.

Batson, R.M., 1995. Cartography, in *Planetary Mapping*, Cambridge Univ. Press, Cambridge, UK, pp. 60–95.

Eliason, E., 1997. Production of digital image models using the ISIS system. *Lunar and Planetary Science,* XXVIII, 331–332.

Gaddis, L.R., Anderson, J., Becker, K., Becker, T., Cook, D., Edwards, K., Eliason, E., Hare, T., Kieffer, H., Lee, E.M., Mathews, J., Soderblom, L, Sucharski, T., and Torson, J., 1997. An overview of the Integrated Software for Imaging Spectrometers (ISIS). *Lunar and Planetary Science*, XXVIII, 387–388.

Gwinner, K., Scholten, F., Giese, B., Oberst, J., Jaumann, R., Spiegel, M., Schmidt, R., Neukum, G., und das HRSC Co-Investigator Team, 2005. Hochauflösende Digitale Geländemodelle auf der Grundlage von Mars Express HRSC-Daten. *Photogrammetrie Fernerkundung Geoinformation*, 5, pp. 387-394.

Gwinner, K., Scholten, F., Spiegel., M., Schmidt, R., Giese, B., Oberst, J., Jaumann, R., Neukum, G., and the HRSC Co-Investigator Team, 2006. Derivation and evaluation of high-resolution digital terrain models from Mars-Express HRSC data. *Photogrammetric Engineering & Remote Sensing*, submitted

Heipke, C., Oberst, J., Attwenger, M., Dorninger, P., Ewe, M., Gehrke, S., Gwinner, K., Hirschmüller, H., Kim, J.R., Kirk, R.L., Lohse, V., Mayer, H., Muller, J.-P., Rengarajan, R., Schmidt, R., Scholten, F., Shan, J., Spiegel, M., Wählisch, M., Yoon, J.-S., Neukum, G., and the HRSC Co-Investigator Team, 2006. The HRSC DTM test. *International Archives of Photogrammetry, Remote Sensing and Spatial Information Sciences*, Vol. XXXVI. Part 4.

Kirk, R.L. 1987. A fast finite-element algorithm for two-dimensional photoclinometry. Ph.D. Thesis, Caltech, Part III, pp. 165–258.

Kirk, R.L., Barrett, J.M., and Soderblom, L.A., 2003a. Photoclinometry made simple…?. ISPRS Working Group IV/9 Workshop "Advances in Planetary Mapping 2003", Houston, March 2003, online at http://astrogeology.usgs.gov/Projects/ISPRS/Meetings/Houston2003/abstracts/Kirk_isprs_mar03.pdf.

Kirk, R. L., Howington-Kraus, E., Redding, B., Galuszka, D., Hare, T. M., Archinal, B. A., Soderblom, L. A., and Barrett, J. M., 2003b, High-resolution topomapping of candidate MER landing sites with Mars Orbiter Camera Narrow-Angle images. *Journal of Geophysical Research,* 108(E12), 8088, doi:10.1029/2003JE002131.

Miller, S.B., and Walker, A.S., 1993. Further developments of Leica digital photogrammetric systems by Helava. *ACSM/ASPRS Convention and Exposition Technical Papers*, 3, pp. 256–263.

Miller, S.B., and Walker, A. S., 1995. Die Entwicklung der digitalen photogrammetrischen Systeme von Leica und Helava. *Zeitschrift für Photogrammetrie und Fernerkundung,* 63(1), pp. 4–16.

Neukum, G., Jaumann, R., and the HRSC Co-Investigator Team, 2004. HRSC: The High Resolution Stereo Camera of Mars Express. *ESA Special Publications* SP-1240.

Scholten, F., Gwinner, K., Roatsch, T., Matz, K.-D., Wählisch, M., Giese, B., Oberst, J., Jaumann, R., and Neukum G., 2005. Mars Express HRSC data processing—Methods and operational aspects. *Photogrammetric Engineering & Remote Sensing*, 71(10), pp. 1143-1152.

Seidelmann, P.K., Abalakin, V.K., Bursa, M., Davies, M.E., De Bergh, C., Lieske, J.H., Oberst, J., Simon, J.L., Standish, E.M., Stooke, P., and Thomas, P.C., 2002. Report of the IAU/IAG Working Group on Cartographic Coordinates and Rotational Elements of the Planets and Satellites: 2000. *Celestial Mechanics and Dynamical Astronomy,* 82, pp. 83–110.

Smith, D.E, et al., 2001. Mars Orbiter Laser Altimeter: Experiment summary after the first year of global mapping of Mars. *Journal of Geophysical Research*, 107, pp. 23689–23722.

Torson, J., and Becker, K., 1997. ISIS: A software architecture for processing planetary images. *Lunar and Planetary Science*, XXVIII, pp. 1443–1444.

Zhang, B., and Miller, S., 1997. Adaptive Automatic Terrain Extraction. *Proceedings of SPIE, Volume 3072, Integrating Photogrammetric Techniques with Scene Analysis and Machine Vision* (edited by D. M. McKeown, J. C. McGlone and O. Jamet). pp. 27-36.